

Behavior of a hydrocarbon liquid dripped onto the surface of a flowing water layer

YOSHINOBU ISHIKUBO,† KENJI ISHIDA and YASUHIKO H. MORI‡

Department of Mechanical Engineering, Keio University, 3-14-1 Hiyoshi,
Kohoku-ku, Yokohama 223, Japan

(Received 5 April 1991 and in final form 18 June 1991)

Abstract—Experimental work is described in which a hydrocarbon liquid (n-octane or n-pentane) is dripped onto the surface of water flowing in a horizontal, rectangular channel that simulates each tray in a multi-tray, direct-contact evaporator. A pair of laterally-finned barriers facing each other is set on the water surface along the channel axis so that floating lenses of the hydrocarbon liquid are forced to make shape oscillations while being conveyed by the substrate water. A promotion of the evaporation of pentane lenses due to the oscillations is examined.

1. INTRODUCTION

THE WORK described in this paper is concerned with a particular type of direct-contact evaporator characterized by a spraying (or dripping) of a volatile oily liquid, such as a light hydrocarbon, onto the surface of an aqueous heat-source liquid such as geothermal brine, solar-pond brine, or industrial waste water. This type of evaporator is expected to suffer less from the scale formation on, and/or corrosion of, the injection ports for the oily liquid than the alternative type, characterized by submerged injection ports [1]. Another superiority of the former type is that it suffers no reduction of the effective temperature driving force for evaporation due to the hydrostatic head of the heat-source liquid. It has been confirmed experimentally that a small drop of some hydrocarbon, or fluorocarbon, liquid dripped in an appropriate way onto the surface of quiescent, not-too-hot water takes the form of a thin biconvex lens floating on the surface without being separated from it by a vapor film [2, 3]. The evaporation of such lenses, due to the heat transfer from the substrate water, has been studied both experimentally and theoretically [2, 4–9]. However, in practical evaporators having, for example, a multi-tray tower configuration, an oily liquid to be vaporized is fed onto the surface of a heat-source liquid which is not stagnant but flowing over each tray and flooding at its downstream end. The surface must be continuously extended and renewed, and thereby causing the oily liquid to show a spreading behavior different from that observed on a stationary water surface. (In fact, Hirahaya *et al.* [10] observed that R113 fed onto the flowing water surface did not

always turn into discrete, circular lenses, but sometimes spread into thinner films having irregular contours.)

The present work aims to investigate the fluid-mechanical and surface-chemical aspects of the process of evaporation of a hydrocarbon liquid dripped onto the surface of water slowly flowing on each horizontal, or slightly inclined, tray installed in a multi-tray tower direct-contact evaporator. Of particular interest in the work is a device that possibly yields an enhancement of the heat transfer to, and the evaporation of, the hydrocarbon liquid so far as it takes the form of discrete lenses. The device conceived is a set of laterally-corrugated, or finned barriers, to be so arranged on the water surface along the longitudinal axis of each tray that they divide the surface into narrow lanes, each of which changes periodically in width along the axis. Each lens of the hydrocarbon liquid is expected to exhibit a periodical shape oscillation, as it flows through one of the lanes, because of some viscoelasticity of the water surface [11], a gravitational effect due to the water menisci formed on the barrier walls, and/or a hydrodynamic effect due to the substrate water beneath the lens. (More details of the possible mechanisms of shape oscillations of lenses are given in the Appendix.) The oscillations of lenses and/or related oscillatory motions of the surface layer of the substrate water presumably induce some secondary convection in the water, causing an enhancement of the heat transfer from the water to the lenses.

The only preceding work that studied an artificial enhancement of the lens evaporation is the one by Mori and Endo [12]. They demonstrated an active enhancement technique that utilized a dilational viscoelasticity of the water surface surrounding a hydrocarbon-liquid lens to make the lens undergo periodical expansion/shrinkage. A motive of the present work is to develop an alternative enhancement

† Current address: Equipment Design Development Research Laboratory, Hitachi Metals Co., Ltd, 5200 Mikajiri, Kumagaya-shi, Saitama-ken 360, Japan.

‡ Author to whom all correspondence should be addressed.

NOMENCLATURE

D	equivalent circular diameter of lens		temperature at which the sum of vapor pressures of pentane and water equals the pressure in the test channel
D_x, D_y	axes of a lens parallel and normal to the channel axis	\bar{u}	average flow velocity of substrate water
l	length of each fin on the barrier	V	volume of lens
p	pitch of fins aligned on the barrier	w	distance between fin tips opposing each other
t	time	x	distance measured along the channel axis.
t_v	evaporation time of lens		
ΔT	excess of water inlet temperature above the		

technique which is much easier to apply to evaporators for practical use.

2. EXPERIMENTAL

The experimental setup used in this work is schematically illustrated in Fig. 1. The setup consisted of a closed loop for circulating water through a test channel and assemblies for feeding to the channel a hydrocarbon liquid cocurrently with the water, and the vapor of the same substance countercurrently. The channel was a model of each tray installed in multi-tray-type direct-contact evaporators. It was so constructed, by welding plates and pipes of transparent PMMA (poly(methylmethacrylate)), as to be integral with the constant-temperature water jacket (see Fig. 2). The channel had a 'raised bottom' extending the full width, 140 mm, of the channel and 600 mm in length. A space 70 mm in height was left between the 'raised bottom' and the top cover plate of the channel. A small bottom portion (4–6 mm in thickness) of the space was occupied with a water layer exhibiting a nearly two-dimensional, laminar flow, while the rest was occupied with a stagnant air or a moderately superheated vapor of hydrocarbon flowing counter-

currently to the water layer at a velocity so low as to hardly promote rippling at the water surface. A pair of PMMA or Teflon barriers (Fig. 3) were so hung from three PMMA bridges spanning the channel that their lower edges just contacted the water surface. A hydrocarbon liquid was dripped onto the water surface from a capillary glass nozzle standing out in the well at the upstream end in the channel. As each drop of the hydrocarbon liquid impinged on the water surface, it immediately turned into a lens or, contrary to our expectation, a much thinner irregularly-shaped film, which then drifted into the lane between the barriers.

The barriers we first prepared were thin PMMA plates plastically deformed into 'folding screen' geometries. To facilitate the working, however, we then replaced them by 'comb-toothed' barriers each consisting of vertically-oriented rectangular fins welded, or screwed, in a row onto a plane strip of PMMA or Teflon. A fully constructed set of such barriers is shown in Fig. 3. The dimensions characterizing the geometries of each set of barriers are defined in Fig. 4.

It is noteworthy that the influence of the barriers on the lens motion observed in a particular experiment

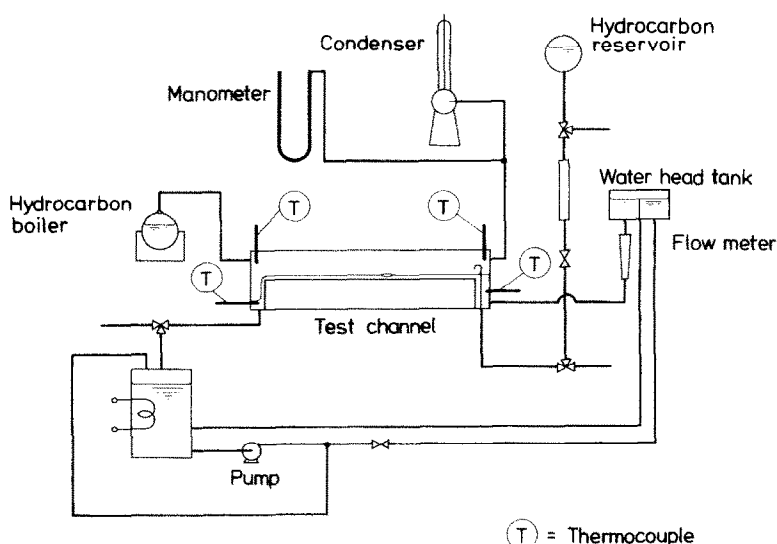


FIG. 1. Experimental setup.

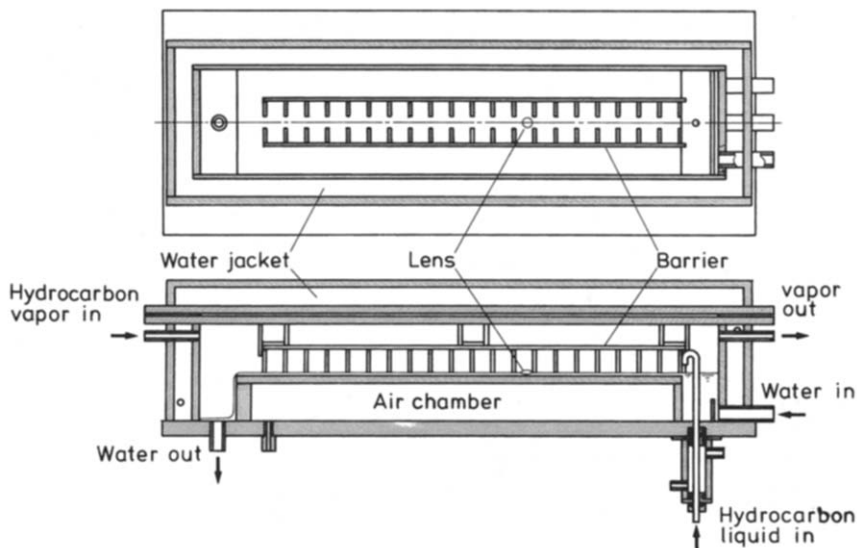


FIG. 2. Plan (top) and side (bottom) views of the test channel integrated with a constant-temperature water jacket.

is not only dependent on their geometry and material, but also on the procedure of their setting prior to the experiment. Illustrated in Fig. 5 are two different procedures, I and II, in which we contrived to maximize and minimize, respectively, the height of water menisci formed on the barrier fins. The larger the contact-angle hysteresis inherent to the water/barrier-

material combination is, the more significant must be the difference in the menisci height thus provided.

The hydrocarbons selected in the experiments were *n*-octane and *n*-pentane. It is unlikely that *n*-octane is actually used in some industrial processes to be vaporized, because of its low volatility; but for the same reason, *n*-octane was found favorable for our

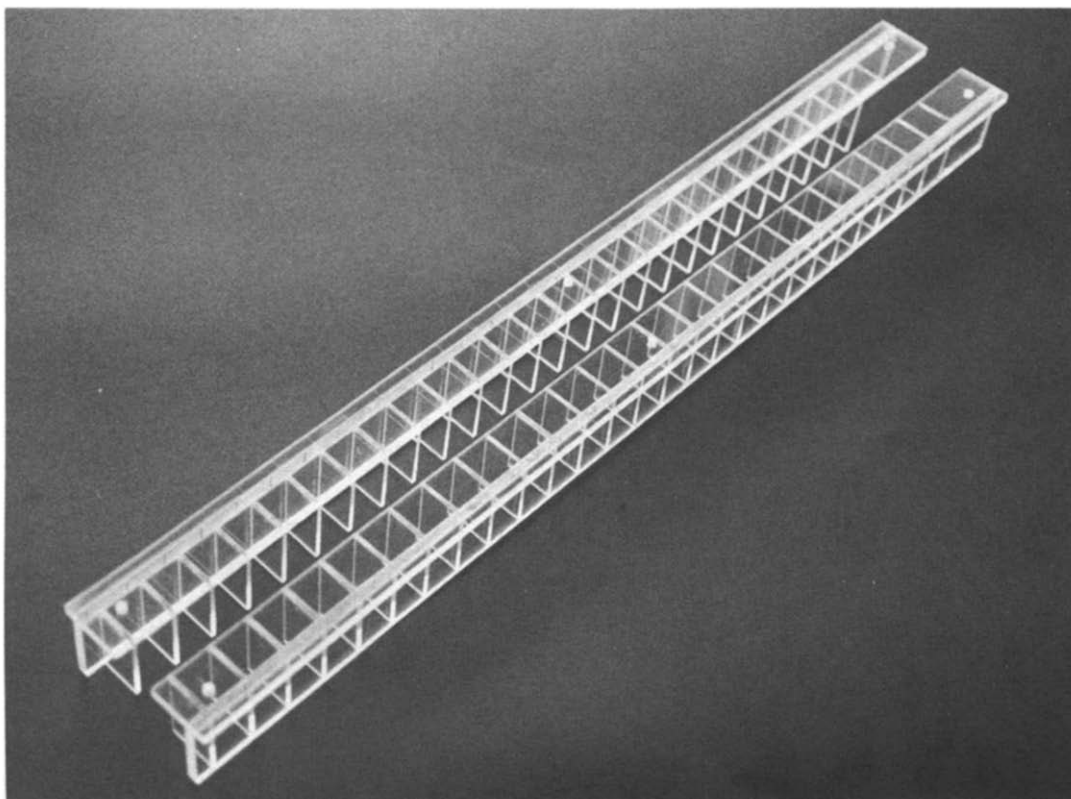


FIG. 3. A typical set of finned barriers made of PMMA plates 2 mm thick.

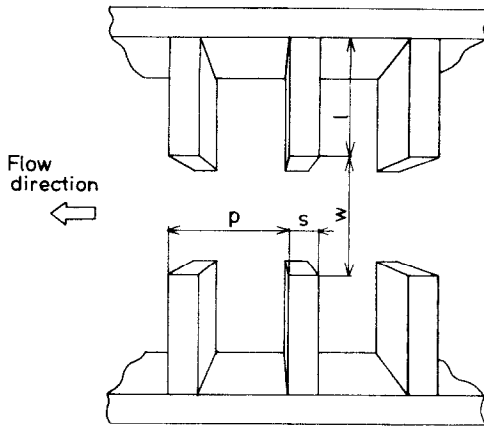


FIG. 4. Plan-view illustration of finned barriers set in the test channel.

close observations of dynamic behavior of lenses. A reagent of 97 wt% certified purity was used, together with tap water, for investigating the effects, on the lens behavior, of the geometry and the material of the barriers, the procedure of barrier setting before each experiment, the water flow rate, etc. Throughout the experiments with *n*-octane and tap water, the channel was kept open to the laboratory air, and no octane vapor was supplied from the external boiler to the channel. No thermal control was made in the experimental setup, while the laboratory air was conditioned to 25 ± 1 °C. Another class of experiments was made with *n*-pentane of 99 wt% certified purity coupled with deionized/distilled water for studying the evaporation of pentane lenses. The water was preheated, before going into the channel, to a temperature moderately higher than T_s , a temperature at which the sum of the saturated-vapor pressures of *n*-pentane and water equals the pressure in the channel,

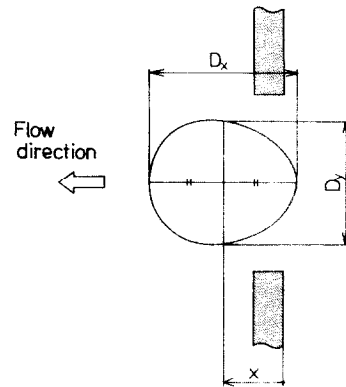


FIG. 6. Definitions of axial and lateral dimensions and axial location of a lens.

which was approximated well by the pressure in the laboratory. The pentane vapor was fed into the channel after being superheated to a temperature slightly exceeding the water temperature.

Each experimental run was accomplished by recording a plan view of a hydrocarbon lens flowing in the lane between the barriers. This was done with a high-speed video camera, at 200 fps, which was mounted on a 'roller coaster' movable along the channel axis. The video recording permitted us to know the variations of x , the distance measured in the flow direction from the front of a particular fin to the center of a lens of interest, and of two perpendicular axes of the lens (see Fig. 6).

3. RESULTS AND DISCUSSION

3.1. Behavior of octane lenses

Octane was found to form stable lenses irrespective of the flow velocity of the water surface as well as

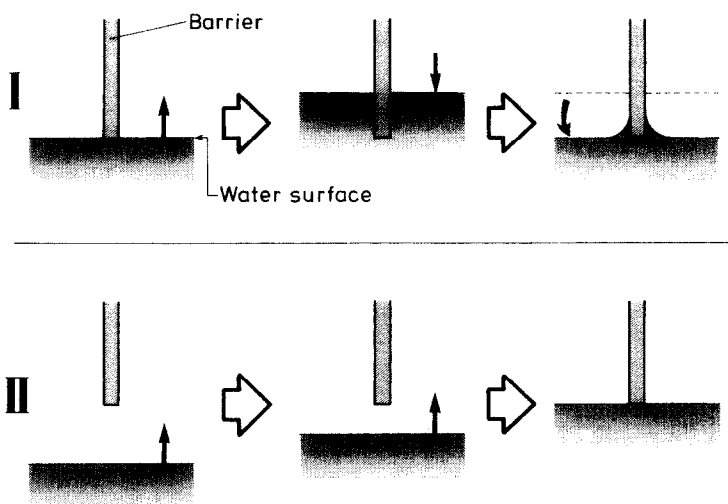


FIG. 5. Alternative procedures of barrier setting: (I) the water surface was once raised to an excessively high level and then lowered to the level of the lower edges of the barriers; (II) the water surface was raised until it just touched the lower edges of the barriers and then stopped.

the feeding rate of the octane sample onto the water surface. First observed were deformations of octane lenses while passing through a 'throat' formed by a pair of barriers each having a single fin (see Fig. 7). The results obtained in this class of experiments are summarized in Figs. 8–10; they are discussed below in order.

Compared in Fig. 8 are lens deformations observed with different barrier settings—(a) vs (b)—and with different barrier materials—(a) vs (c). Clearly the most distinct deformation was observed when barriers made of the less hydrophobic material, PMMA, were set on the water surface via procedure I and hence the three-phase contact line on each barrier wall was elevated the highest above the level water surface. This fact indicates a dominant hydrostatic effect of the water menisci on the lens deformations. All of the results given in later figures were obtained exclusively with PMMA barriers set in procedure I. Besides, the specifications of s to D , given in the caption to Fig. 8, apply for later figures as well, unless otherwise noted.

Each lens takes the minimum in D_y/D_x during or just after its passage through the 'throat' formed by the fins; and then takes the maximum, as it flows away from the 'throat', showing a damped oscillation of its shape. The variations of these extreme values in D_y/D_x with the fin thickness, s , and with the width of the 'throat', w , are plotted in Figs. 9 and 10. Here we note that the magnitude of the deformation of lenses, $(D_y/D_x)_{\max} - (D_y/D_x)_{\min}$, is maximized at a particular fin thickness, which seems to be approximately 8 mm in Fig. 9, but will increase with an increase in the water flow velocity, \bar{u} . In a separate experiment, we observed that octane lenses, each 59 mm^3 in volume, took the form $D_y/D_x = 0.68 \pm 0.06$ when equilibrated on a stagnant water surface bordered by a pair of parallel PMMA plates, 14 mm apart from each other, which may be viewed as barriers with $s \rightarrow \infty$. The above value of D_y/D_x is approximated by the values of $(D_y/D_x)_{\min}$ in the range $s \geq 5 \text{ mm}$ (Fig. 8); this is more evidence that the apparently dynamic deformations of flowing lenses are primarily ascribable to the static effect of the water menisci.

Whenever the lens diameter D is fixed, the deformation becomes more prominent with a decrease in w/D (Fig. 10). It should be noted, however, that the deformation is not similar with respect to w/D . In fact, the set of data for $w/D = 1.54$ indicates that the magnitude of the deformation is maximized with lenses of an intermediate size; larger lenses are less affected by the water menisci because of a larger distance kept between the periphery of each of the lenses and the fin tips, while smaller lenses, considerably rigidified by larger capillary pressures across their surfaces, can resist a larger effect of the menisci without being distorted largely.

The ranges of l and \bar{u} covered by the experiments with single-fin barriers were 10–30 mm and 18–35 mm s^{-1} , respectively. No appreciable change in the lens deformation with l or \bar{u} was observed.

Three pairs of PMMA multi-fin barriers having different pitches were constructed for use in another class of experiments to be done under the same conditions for s to D specified in the caption to Fig. 8 and barrier-setting procedure I, except that w could be other than 18 mm. The selection of the pitches was based on the oscillatory behavior of lenses observed with single-fin barriers under the corresponding conditions: the behavior is represented, together with axial distances characterizing the behavior, in Fig. 11. The three pitches selected were equal to $x_1 - x_2$ ($= 18.0 \text{ mm}$), x_1 ($= 27.5 \text{ mm}$), and $x_1 + x_2$ ($= 36.5 \text{ mm}$). The behavior of octane lenses observed with the multi-fin barriers thus designed is shown in Fig. 12. As expected, the amplitude of shape oscillations of the lenses was maximized when the pitch equalled x_1 , while the sensitivity of the amplitude to the pitch seems to vary with w .

3.2. Behavior of pentane and enhancement of its evaporation

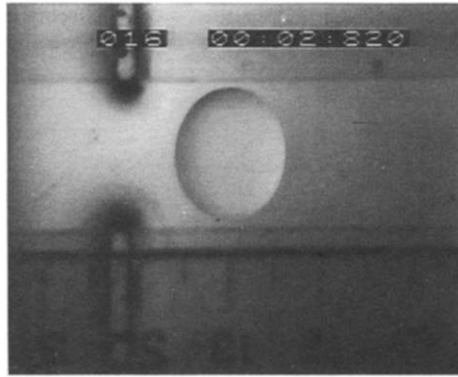
The dripping of pentane liquid from only one nozzle located at the upstream end in the test channel (Fig. 2) did not result in the formation of stable lenses, but provided irregularly shaped films or rafts exhibiting amoeboid movements while flowing in the lane between barriers. Such behavior of pentane liquid hardly changed, even if the flow rate of the pentane vapor and that of the pentane liquid issuing from the nozzle are raised considerably.

Qualitatively speaking, the above-mentioned observation is consistent with the conventional notion, supported by some surface-chemical investigations [13, 14], that n-alkanes tend to become increasingly spreadable on a water surface with a decrease in the number of carbon atoms in the molecule. Recent studies by Mori *et al.* [15] and Endoh *et al.* [16] estimated the equilibrium spreading coefficient of n-pentane on water at -0.08 to -0.04 mN m^{-1} under the pressure of 101.3 kPa. This means that only a minute extension of the water surface may change the sign of the spreading coefficient on the surface and thereby cause pentane to spread over the surface instead of being constricted into lenses.

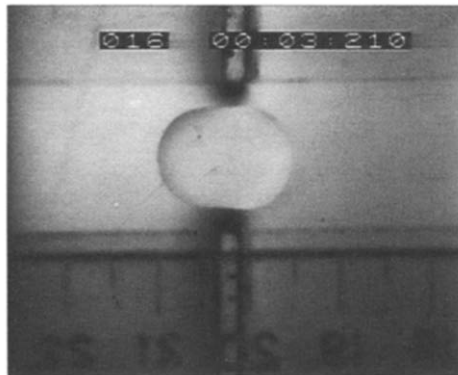
In the present experiments, the water surface was continuously expanded and renewed, since the water was poured over the end of the channel. Therefore, the behavior of pentane liquid was dependent on the rate of expansion/renewal of the water surface relative to the rate of adsorption of pentane molecules onto the surface. Evidently, the adsorption from the vapor phase alone was insufficient to keep the number density of adsorbed pentane molecules on the water surface at a level high enough to constrict pentane liquid into lenses.

The tendency of pentane liquid to spread on the water surface rather than remain as lenses may be a favorable factor for the purpose of enhancing the evaporation. However, the tendency to spreading will be subdued in evaporators in practical use in which

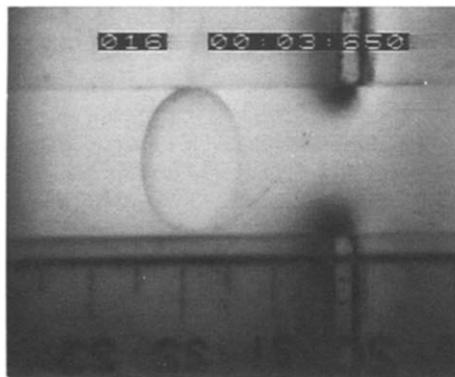
Flow
direction
←



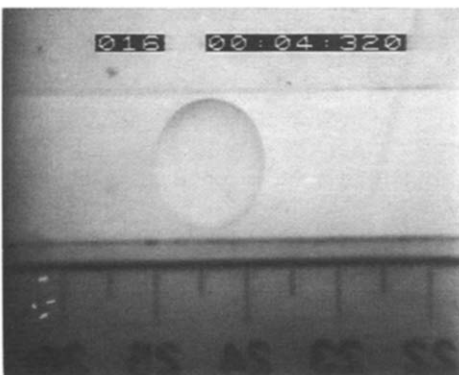
t = 0s



0.39s



0.83s



1.50s

FIG. 7. Videograms showing a sequence of passing of an octane lens through a 'throat' formed by a pair of single-fin barriers.

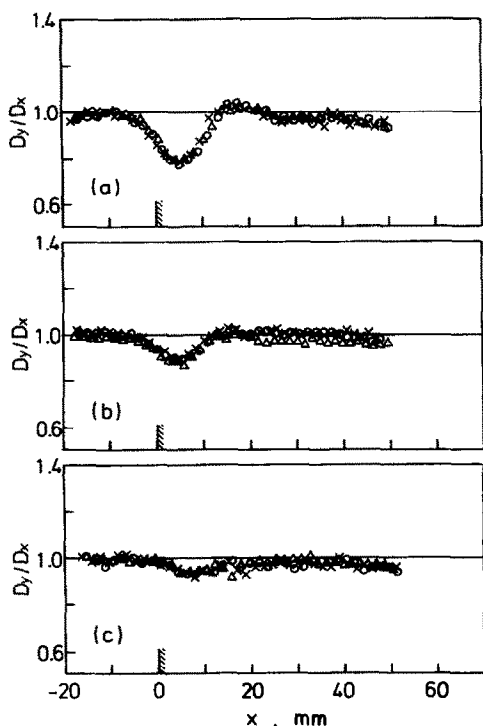


FIG. 8. Comparisons of lens deformations observed with single-fin barriers made of different materials and set via different procedures. $s = 2$ mm, $l = 20$ mm, $w = 18$ mm, $\bar{u} = 27$ mm s^{-1} , $V = 59$ mm 3 , and $D = 11.7$ mm. (a) PMMA barriers set via procedure I; (b) PMMA barriers set via procedure II; (c) Teflon barriers set via procedure I. In each graph, data on three different sample lenses are plotted.

pentane liquid is sprayed from closely arranged nozzles at a considerably high rate per unit area of the water surface, possibly resulting in a quite high rate of replenishment of pentane molecules onto the water surface via surface diffusion from the pentane liquid phase. For approximating such a practical con-

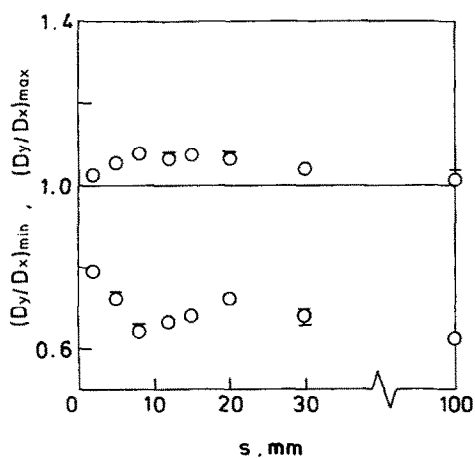


FIG. 9. Effect of barrier thickness s on the maximum lens distortion. Each open circle represents the average of three independent data obtained with different sample lenses, while the scatter range of the data is indicated by the vertical bar on the circle unless the range is narrower than the diameter of the circle.

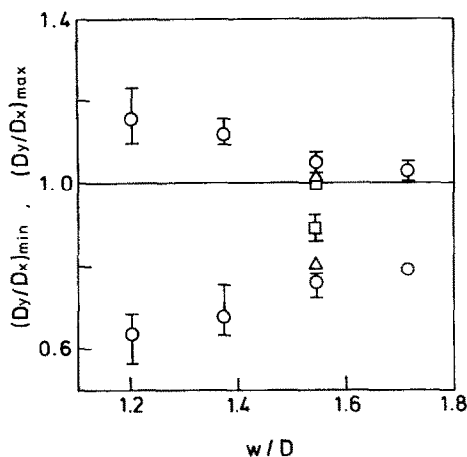


FIG. 10. Effect of the distance between the tips of fins opposed to each other, w , on the maximum lens distortion. Δ , $D = 7.0$ mm; \circ , $D = 11.7$ mm; \square , $D = 20.9$ mm.

dition, we installed two additional nozzles at both sides of the primary nozzle so that pentane liquid was fed not only onto the central lane between the barriers but also onto the side lanes behind the barriers. The flow rate of pentane liquid per nozzle was raised up to 171–195 mm 3 s^{-1} , while \bar{u} was reduced to 18 mm s^{-1} , in order to elevate the number density of pentane molecules adsorbed on the water surface at each instant. As a result of the expedient stated above, we succeeded in observing each of the pentane lenses flowing in line until it completely evaporated away, and thereby determining its evaporation time t_e —i.e. the lapse of time between its formation and vanishing.

Two kinds of barriers were used in this class of experiments: finned barriers ($s = 2$ mm, $l = 20$ mm, $p = 10$ mm, $w = 10$ mm) and plane-surface barriers, 14 mm apart from each other, the latter serving only to insulate the central lane in the channel from undesirable disturbances from the side lanes. Variations in D_y and D_y/D_x of a lens during its passage through the lane bordered by the finned barriers are exemplified in Fig. 13. It is seen there that the amplitude of the oscillation of the pentane lens is rather small

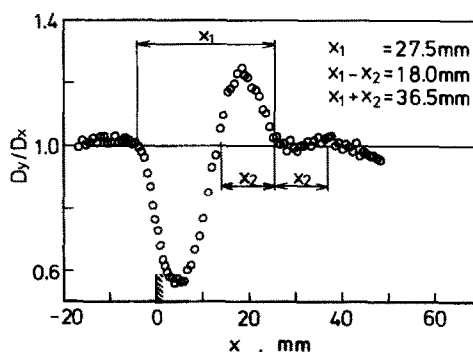


FIG. 11. Axial distances characterizing oscillatory motion of an octane lens passing by a pair of single fins. $w = 14$ mm.

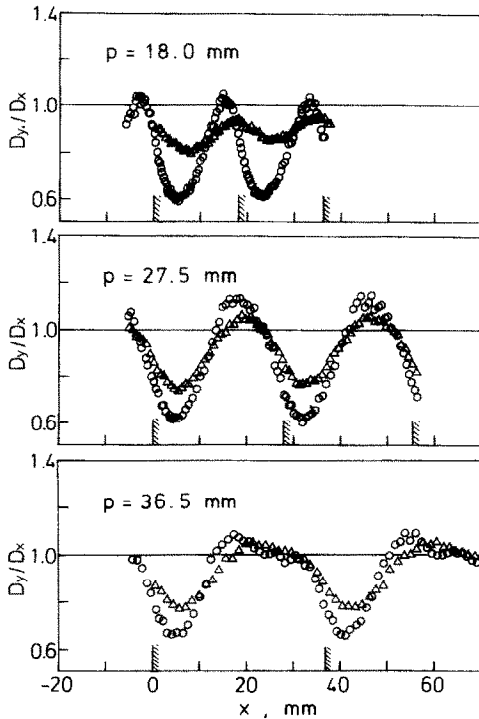


FIG. 12. Oscillatory behaviors of octane lenses observed with multi-fin barriers. \circ , $w = 14$ mm; \triangle , $w = 18$ mm.

compared to those of octane lenses demonstrated in Fig. 12. Two reasons come to mind: (a) pentane lenses are much thinner than octane lenses and hence their geometrical response to any external-force change is much slower; and (b) the geometry of the finned barriers used is not optimized for pentane lenses that have longer response time, as just mentioned, and reduce while moving along the barriers.

Compared in Table 1 are the evaporation time t_v , for pentane lenses of 8–10 mm in initial diameter, measured under the use of the plane-surface barriers,

Table 1. Evaporation time of pentane lenses of 8–10 mm in initial diameter. $\bar{u} = 18$ mm s⁻¹, $\Delta T = 16.3$ K

Plane-surface barriers	12.3 ± 2.3 s ($\sim 95\%$ coverage)
Finned barriers†	8.2 ± 2.4 s ($\sim 95\%$ coverage)

† Consult caption to Fig. 13 regarding the barrier geometry.

and those measured under the use of the finned barriers. The extent of the reduction in t_v in the presence of the finned barriers was about 30%. The reduction may be increased by modifying the geometry of the barriers. It seems desirable that both p and w not be constant, but variable along the channel axis to accommodate themselves to the reduction in lens diameter.

4. CONCLUDING REMARKS

Through the present work, it has been confirmed that shape oscillations of liquid lenses can be induced by setting regularly-jagged barriers on the surface of a flowing substrate liquid and that the shape oscillations thus obtained can enhance the convective heat transfer from the substrate liquid to the lenses and thereby accelerate their evaporation. The observations of mechanical behaviors of lenses discussed here will serve as a guide for optimizing the geometry of the barriers serving to excite the lens oscillation in a given lens/substrate system.

We admit, however, that oscillations of lenses actually observed failed to come up to our expectations; the same is true for the magnitude of enhancement of the evaporation. This failure mostly comes from the fact, revealed in this work, that the viscoelasticity of the water surface, possibly covered with a hydrocarbon monolayer, does not work so well to distort lenses as we anticipated.

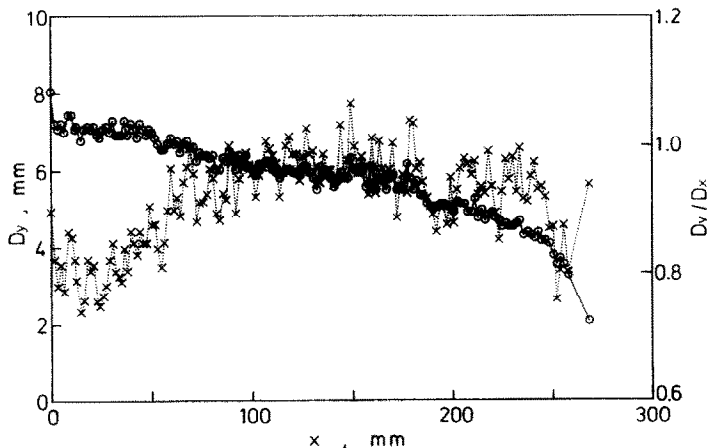


FIG. 13. Variations of D_y (\circ) and D_y/D_x (\times) during the evaporation of a pentane lens after its formation at $x = 0$, $s = 2$ mm, $l = 20$ mm, $p = 10$ mm, $w = 10$ mm, $\bar{u} = 18$ mm s⁻¹, and $\Delta T = 16.3$ K.

It may be worthy of note that an evaporation enhancement will also be attained by another way of using the barriers. Corrugated barriers, for example, can be so arranged as to give zigzag or sinusoidal lanes. Alternatively, finned barriers may be set such that the fins are not aligned but staggered, thus forming labyrinth lanes. Such barrier arrangements will cause each lens to rock from side to side, while the flow in the bulk of the substrate liquid will still remain rectilinear. Larger enhancement of evaporation might be available with those arrangements or with some other variations. Comparative examinations of various barrier arrangements are left to future study.

Acknowledgements—We are indebted to the Energy Fundamentals Division, the Electrotechnical Laboratory, Tsukuba, and to Dr N. Kaji and his students at the Institute of Vocational and Technical Education, Sagamihara, for their kind offices for permitting us to use a high-speed video camera and a video analyzer in their charge. The financial support by the Grant in Aid for Scientific Research from the Ministry of Education, Science and Culture of Japan (Grant 01 550 191) is acknowledged. Some of the experiments dealing with octane lenses were done with assistance of H. Ogawa, then undergraduate at the Department of Mechanical Engineering, Keio University.

REFERENCES

1. H. R. Jacobs, R. S. Deeds and R. F. Boehm, Heat transfer characteristics of a surface type direct contact boiler, ASME Paper 76-HT-26 (1976).
2. M. Bentwich, U. Landau and S. Sideman, Direct contact heat transfer with change of phase: evaporation of discrete volatile films from the surface of a stagnant immiscible liquid, *Int. J. Heat Mass Transfer* **13**, 945–956 (1970).
3. T. Nosoko and Y. H. Mori, Vaporization of drops of a denser, volatile liquid dropped onto a surface of another liquid, *Trans. ASME, J. Heat Transfer* **107**, 384–391 (1985).
4. C. A. Kodres, H. R. Jacobs and R. F. Boehm, Heat transfer to an evaporating, floating lens, ASME Paper 79-HT-13 (1979).
5. C. A. Kodres, H. R. Jacobs and R. F. Boehm, A numerical method for determining direct-contact heat transfer rates to a suspended evaporating floating droplet, *Numer. Heat Transfer* **3**, 21–34 (1980).
6. M. Kaneko and Y. H. Mori, Evaporation of a volatile-liquid lens floating on the surface of a stagnant immiscible liquid, *Int. Commun. Heat Mass Transfer* **11**, 209–218 (1984).
7. T. Nosoko, T. Ohyama and Y. H. Mori, Evaporation of volatile-liquid lenses floating on an immiscible-liquid surface: effects of the surface age and fluid purities in n-pentane/water system, *J. Fluid Mech.* **161**, 329–346 (1985).
8. T. Nosoko and Y. H. Mori, The evaporation of volatile-liquid lenses floating on an immiscible-liquid surface: the effect of convection induced in the substrate liquid, *Proc. 8th Int. Heat Transfer Conf.*, Vol. 4, pp. 1883–1888. Hemisphere, Washington, DC (1986).
9. T. Nosoko, S. Endo and Y. H. Mori, Laser shadow-

graphy and holographic interferometry for visualizing thermal convection induced by direct-contact evaporation of liquid lenses. In *Flow Visualization IV* (Edited by C. V  ret), pp. 67–72. Hemisphere, Washington, DC (1987).

10. K. Hirahaya, T. Nagano and Y. Fujita, Heat-transfer process in direct contact evaporator—3rd report: Behavior and heat transfer of R113 liquid floating on flowing water surface (in Japanese), *Trans. JSME* **B54**, 1814–1819 (1988).
11. M. van den Tempel, Surface rheology, *J. Non-Newtonian Fluid Mech.* **2**, 205–219 (1977).
12. Y. H. Mori and S. Endo, An attempt at enhancing direct contact evaporation utilizing the surface dilational viscoelasticity, *Int. J. Heat Mass Transfer* **31**, 1835–1842 (1988).
13. F. Hauxwell and R. H. Ottewill, A study of the surface of water by hydrocarbon adsorption, *J. Colloid Interface Sci.* **34**, 473–479 (1970).
14. C. del Cerro and G. J. Jameson, The behavior of pentane, hexane, and heptane on water, *J. Colloid Interface Sci.* **78**, 362–375 (1980).
15. Y. H. Mori, T. Nosoko, A. Mikami and T. Ohyama, A practical method for rectifying interfacial tension data to predict the shape of interfaces in an immiscible liquid/liquid/gas system, *Chem. Engng Commun.* **92**, 95–102 (1990).
16. K. Endoh, A. Mikami and Y. H. Mori, Determination of the spreading coefficient of one liquid on another by means of interferometric measurements of liquid-lens thickness, *Colloids Surfaces* **46**, 99–113 (1990).

APPENDIX. MECHANISMS OF LENS DEFORMATION

As a hydrocarbon-liquid lens passes by fins (or some protrusions) on two barriers opposed to each other, it must be subjected, more or less, to three different effects, each of which can cause periodical deformations of the lens. These effects have physicochemical, hydrostatic, and hydrodynamic origins, respectively, as explained below in order.

It is reasonably presumed that each lens is surrounded by a riftless surface film spread over the substrate water. The film is most likely a mixed monolayer of the same substance as that of the very lens and surfactant contaminants inevitably involved in the experimental system. As the film passes through a ‘throat’ formed by two *vis-  -vis* fins, it is sheared and compressed laterally. Due to its viscoelasticity (i.e. dilational viscoelasticity and shear viscosity), the film can exert a two-dimensional pressure as well as a shear on a lens, while they pass together through the throat, causing a transient deformation of the lens into a slender configuration.

The second effect, which was found to be the most pronounced in the present experiments, arises from the menisci formed on the fins. So long as the menisci are concave in an upward direction, a lens located between two *vis-  -vis* fins is forced to become, due to the hydrostatic/capillary force balance, laterally narrower than it would be under no influence of the menisci.

The third effect is provided by the substrate water flow. So far as the barriers are submerged into the water even to a minimal depth, each pair of two *vis-  -vis* fins serves as an orifice, causing a convergent–divergent flow of the water in a near-surface layer, irrespective of the viscoelasticity of the surface. The convergent–divergent flow can possibly be a cause of prolate–oblate deformation of lenses conveyed by the flow.

COMPORTEMENT D'UN HYDROCARBURE LIQUIDE S'EGOUTTANT SUR LA SURFACE D'UNE COUCHE D'EAU EN ECOULEMENT

Résumé—On décrit un travail expérimental relatif à un hydrocarbure liquide (n-octane ou n-pentane) qui s'égoutte sur la surface de l'eau en écoulement dans un canal horizontal, rectangulaire qui simule un arrangement d'évaporateur à contact direct. Une paire de barrières ailetées latéralement se faisant face est disposée à la surface de l'eau le long de l'axe du canal de façon à faire osciller les gouttes d'hydrocarbure flottant pendant leur transport par l'eau. On examine l'amélioration de l'évaporation des "yeux" de pentane pendant les oscillations.

DAS VERHALTEN EINES AUF DIE OBERFLÄCHE EINER STRÖMENDEN WASSERSCHICHT TROPFENDEN FLÜSSIGEN KOHLENWASSERSTOFFS

Zusammenfassung—Es wird eine experimentelle Arbeit beschrieben, bei der ein flüssiger Kohlenwasserstoff (n-Okтан oder n-Pentan) auf die Oberfläche einer strömenden Wasserschicht tropft. Die Versuchsanordnung besteht aus einem waagerechten Rechteckkanal, der einen Ausschnitt aus einem Mehrplatten-Direktkontaktverdampfer darstellt. Auf der Wasseroberfläche ist entlang der Kanalachse ein Paar seitlich berippter Strömungsbarrieren angebracht. Durch diese Anordnung werden schwimmende Kohlenwasserstoff-Linsen zu Formoszillationen angeregt, während sie auf der Wasserschicht transportiert werden. Die Verbesserung der Verdampfung der Pentanlinsen aufgrund der Oszillationen wird untersucht.

ПОВЕДЕНИЕ ЖИДКОГО УГЛЕВОДОРОДА ПРИ ЕГО КАПЕЛЬНОМ НАНЕСЕНИИ НА ПОВЕРХНОСТЬ ДВИЖУЩЕГОСЯ СЛОЯ ВОДЫ

Аннотация—Проводится эксперимент, в котором жидкий углеводород (н-октан и н-пентан) в виде капель наносится на поверхность воды, текущей по горизонтальному каналу прямоугольного сечения, который моделирует каждый из элементов многотарельчатого контактного испарителя. На поверхности воды вдоль оси канала установлена пара обращенных друг к другу перегородок с поперечным оребрением, в результате чего формы плавающих "линз" жидкого углеводорода осциллируют по мере перемещения слоя воды. Исследуется усиление испарения "линз" пентана за счет колебаний.